Atmospheric Environment 189 (2018) 98–106

Contents lists available at ScienceDirect

Atmospheric Environment

journal homepage: www.elsevier.com/locate/atmosenv

Diurnal variation of nanocluster aerosol concentrations and emission factors in a street canyon

Riina Hietikko[a], Heino Kuuluvainen[a], Roy M. Harrison[b,c], Harri Portin[d], Hilkka Timonen[e], Jarkko V. Niemi[d], Topi Rönkkö[a,*]

[a] Aerosol Physics, Faculty of Natural Sciences, Tampere University of Technology, FI-33101 Tampere, Finland
[b] Division of Environmental Health and Risk Management, School of Geography, Earth and Environmental Sciences, University of Birmingham Edgbaston, Birmingham B15 2TT, United Kingdom
[c] Department of Environmental Sciences / Center of Excellence in Environmental Studies, King Abdulaziz University, PO Box 80203, Jeddah 21589, Saudi Arabia
[d] Helsinki Region Environmental Services Authority, FI-00240 Helsinki, Finland
[e] Atmospheric Composition Research, Finnish Meteorological Institute, FI-00101 Helsinki, Finland

ARTICLE INFO

Keywords:
Nanocluster aerosol
Street canyon
Urban air
Traffic emissions

ABSTRACT

Traffic emits a considerable amount of aerosol particles in urban areas and has also recently been shown to be a significant source of sub-3 nm particles. In this study, the concentration of sub-3 nm particles, here referred to as nanocluster aerosol (NCA), was continuously measured with 1 s resolution in a busy street canyon in the city of Helsinki, Finland, for a month period in 2017. NCA concentrations were carefully analyzed with respect to the time of day, the wind direction, the condensation sink, the concentration of sub-7 nm particles, the total particle size distribution, and the CO_2 concentration, from which the emission factors for the NCA were calculated. The concentration of the NCA seemed to follow a similar trend to that of sub-7 nm particles. Diurnal variation of the NCA concentration divided into weekdays and weekends and sorted according to the wind direction followed the amount traffic. The NCA concentration was at highest when wind was blowing directly from the road, during the rush hours or when the condensation sink calculated from the particle size distributions was low. The NCA concentration was in line with the traffic-related nucleation mode of the size distribution and its diurnal variation, and the NCA fraction comprised a relatively large part of the total particle number concentration. Average emission factors for the NCA and sub-7 nm particles were $9.36 \cdot 10^{14}\,kg_{fuel}^{-1}$ and $2.73 \cdot 10^{15}\,kg_{fuel}^{-1}$, respectively. Diurnal variation of the emission factors showed an increase in the night, which may result from a dependency of the emission factors on traffic composition, temperature, condensation sink or the driving mode of vehicles.

1. Introduction

Exhaust emitted by road traffic contains particles in a wide particle size range. These particles are frequently seen in particle size distribution as separate modes, referred to as a nucleation mode (mean particle size 10–30 nm) and an accumulation mode (mean particle size 30–100 nm) (Shi and Harrison, 1999). In addition to their size, particles in different modes have different physical and chemical characteristics; the accumulation mode, in exhaust studies also called the soot mode, is comprised of solid agglomerated soot particles consisting of elemental carbon with sulfuric and organic species condensed on their surfaces, while the particles in the nucleation mode are comprised mainly of semi-volatile compounds (Biswas et al., 2007). Information on the chemical composition of the nucleation mode particles is limited. Organic compounds in the range of C_{17}-C_{25} (Tobias et al., 2001) and C_{24}-C_{32} (Sakurai et al., 2003) have been reported, and Alam et al. (2016) reported concentrations of specific n-alkanes, n-alkylcyclohexanes and PAH, the former as a function of particle size. The semi-volatility has been demonstrated by partitioning between the condensed and vapour phases (Alam et al., 2016). Some studies have shown the presence of an involatile core within nucleation mode particles (Rönkkö et al., 2007; Kirchner et al., 2009). Shi and Harrison (1999) presented evidence for the presence of sulphate and Kirchner et al. (2009) reported spots of 1–3 nm with very high contrast under a Transmission Electron Microscope, strongly suggestive of metallic constituents. Alanen et al. (2015) detected particles with a non-volatile core from natural gas engine exhaust in the same size range.

A recent study by Rönkkö et al. (2017) showed that traffic is a major source of nanocluster aerosol (NCA), i.e. particles with a diameter smaller than 3 nm. Also Kontkanen et al. (2017) studied the

* Corresponding author.
E-mail address: topi.ronkko@tut.fi (T. Rönkkö).

https://doi.org/10.1016/j.atmosenv.2018.06.031
Received 20 March 2018; Received in revised form 17 June 2018; Accepted 19 June 2018
Available online 22 June 2018

concentrations of sub-3 nm particles in various environments around the world and noticed the concentrations to be higher in areas with anthropogenic emissions. These observations would not have been possible without the recent development of instrumentation able to detect the sub-3 nm particles (Iida et al., 2009; Vanhanen et al., 2011). The existence of sub-3 nm particles is not surprising based on the previous knowledge of particle size distributions and number concentrations in urban areas and traffic sites (Zhu et al., 2002; Xiao et al., 2015), but the recent observations of urban and traffic-related NCA have still been significant with respect to the current understanding of urban aerosols.

Usually the existence of sub-3 nm particles in the atmosphere has been associated with new particle formation events (Kulmala et al., 2007b; Kirkby et al., 2016). An atmospheric new particle formation event is a process that requires the presence of gas phase components with low vapor pressure, and the role of photochemistry has been considered essential in the production of these components (Kulmala and Kerminen, 2008). However, Kontkanen et al. (2017) found that the high concentrations of sub-3 nm particles in urban areas were not directly linked to the growth of larger particles, which is usually the case in atmospheric new particle formation events. Rönkkö et al. (2017) reported that the concentrations of NCA depended highly on the vicinity and diurnal patterns of traffic, as well as on the type of the traffic environment and on the driving mode of vehicles. By using ambient CO_2 measurements, they were able to determine emission factors for NCA ranging from $2.4{\cdot}10^{15} \pm 1.5{\cdot}10^{15}\ kg_{fuel}^{-1}$ to $2.9{\cdot}10^{15} \pm 0.5{\cdot}10^{15}\ kg_{fuel}^{-1}$. Rönkkö et al. (2017) suggested the concept of delayed primary aerosol to describe the most probable pathway for the formation of NCA, where particles are formed from precursor gases existing in hot exhaust during a relatively fast cooling and dilution process on a time scale of a few seconds. This pathway differs from the secondary aerosol formation in which photochemical reactions and oxidation processes lower the volatility of gaseous compounds before the gas-to-particle conversion. The time scales of the secondary aerosol formation usually range from hours to several days in the atmosphere. Altogether, it is possible that the urban NCA is a combination of particles formed via both of these pathways. It may also contain solid primary particles which have been detected previously in the size range above 3 nm (Sgro et al., 2008; Rönkkö et al., 2013), for natural gas engines also in the size range below 3 nm (Alanen et al., 2015; Lehtoranta et al., 2017).

In urban areas, street canyons are important micro-environments with respect to the dispersion of traffic-generated aerosols and human exposure. Usually, the highest particle concentrations within urban areas are measured in street canyons with congested traffic (Kumar et al., 2011), and these environments play a key role in understanding the effect of anthropogenic emissions on regional air quality (Monks et al., 2009). In the study of Rönkkö et al. (2017), one of the measurements of NCA was conducted in an urban street canyon environment, where they measured NCA concentrations with a single combination of a particle size magnifier (PSM) and a condensation particle counter (CPC). PSM is an instrument capable of growing particles even as small as approximately 1 nm to detectable sizes with diethylene glycol (Vanhanen et al., 2011). In Rönkkö et al. (2017), the PSM was operated in a step mode where four different cut-off sizes were alternated through changing the saturator flow rate of the PSM. One step lasted for 1 min and the total cycle was thus 4 min. However, the traffic-originated concentrations measured on the kerbside change constantly and rapidly, so better time resolution is required for connecting NCA concentrations with simultaneous traffic situations. Measuring concentrations simultaneously with several instruments with different cut-off sizes gives more precise information on the fraction of NCA (Kulmala et al., 2007a; Pirjola et al., 2017).

The influence of the urban NCA on air quality and public health is not straightforward but most likely significant. Fine particles have been confirmed to pose significant risks to human health by causing cardiovascular diseases and increasing mortality (Lelieveld et al., 2015; Pope et al., 2002). The mechanisms affecting human organs are still largely unknown. Several studies have established a connection between the toxicity of nanoparticles and the interaction of their surface with the alveolar region of the lung (Nemmar et al., 2002; Oberdörster et al., 2005). In this respect, the sub-3 nm particles may not be the worst problem because a majority of these small particles is deposited into the upper airways of the respiratory tract due to diffusion. However, these particles are prone to coagulate with particles more efficiently entering the alveolar region of the lungs. The traffic-related soot mode is highly elevated in the lung deposited fraction of particulate matter in urban areas (Kuuluvainen et al., 2016). Another recently introduced concern is that small particles may enter the brain directly through the olfactory nerve and cause neurodegenerative diseases (Maher et al., 2016). This concern is most likely relevant for NCA particles if they appear to be insoluble.

The impacts of aerosol particles on climate are complex, causing both cooling and warming, and despite numerous studies are not yet precisely quantified. Particles affect climate both directly and indirectly, for example, through radiative forcing and cloud formation (Haywood and Boucher, 2000; Rotstayn et al., 2009). Rönkkö et al. (2017) showed through particle number emission factors that the contribution of the traffic-related NCA to global anthropogenic particle number emissions was significant. Even though the full effects of recently discovered NCA on the urban aerosol are largely unknown, it is clear that these small particles take part in new particle formation events, particle growth through coagulation, and other atmospheric processes within urban areas.

In this study, the effect of traffic on NCA concentrations was studied in an urban street canyon environment with a better time resolution and more precise measurements than before. Stationary measurements in an urban street canyon lasted for a month and produced important information on particles that humans are continuously exposed to. The measurement of NCA was based on a particle size magnifier (PSM) that was operated in the fixed mode in parallel with condensation particle counters, all measuring with a time resolution of 1 s, to obtain real-time concentrations of NCA. This study extends the observations of NCA and introduces some new aspects, for example, the diurnal variation of emission factors. Along with NCA, also the concentration of sub-7 nm particles and total particle concentration were studied.

2. Experimental

The measurements for this study were carried out in Helsinki at an urban supersite measurement station (Mäkelänkatu 50) operated by the Helsinki Region Environmental Services Authority (HSY) in May 2017. Apart from short maintenance breaks, data were continuously measured from May 2nd to June 1st. The measurement station is located in a street canyon at the kerbside of one of the main streets of the city. According to traffic count in an intersection near the measurement station, an average of 29 000 vehicles drove along the street every weekday and 19 000 every weekend day during the measurement campaign (traffic data from the City of Helsinki). The street consists of six lanes, two rows of trees, two tramlines and two pavements, resulting in a total width of 42 m.

The measurement setup consisted of two condensation particle counters (TSI CPC 3776 and Airmodus CPC A20) and one combination of a particle size magnifier (Airmodus PSM A10) and a condensation particle counter (Airmodus CPC A20), here simply referred to as a PSM. The cut-off sizes of the instruments are listed in Table 1. The CPC A20 counted particles with a diameter greater than 7 nm whereas the CPC 3776 measured particles above 3 nm. The PSM was operated in a fixed mode with a constant saturator flow of 1.3 lpm detecting particles as small as approximately 1 nm. The instruments measured particle number concentration from an outdoor air sample simultaneously, so the fraction of nanocluster aerosol (NCA) could be obtained from the difference of the CPC 3776 and the PSM data, and the fraction of sub-7

Table 1
Cut-off sizes of the particle size magnifier (PSM) and the condensation particle counters (CPC). The concentrations of the NCA and sub-7 nm particles were obtained by subtracting the data of the CPCs from the data of the PSM.

Instrument	Cut-off size
Airmodus PSM A10 + Airmodus CPC A20	1 nm
TSI CPC 3776	3 nm
Airmodus CPC A20	7 nm

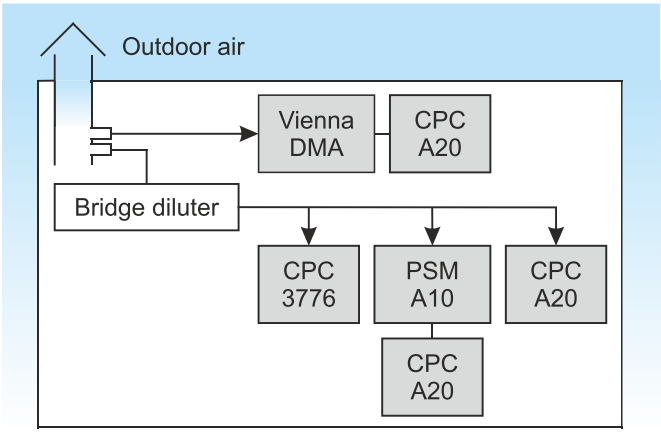

Fig. 1. The measurement setup. The outdoor air sample was drawn from the roof into the measurement station, diluted with a bridge diluter and conducted to the condensation particle counters (CPCs) and particle size magnifier (PSM). The differential mobility particle sizer (DMPS) was connected to a separate sampling line before the bridge diluter.

nm particles similarly from the CPC A20 and the PSM data.

All the instruments were positioned inside the measurement station as close to each other as possible and connected to the same sampling line. The outdoor air sample was drawn from the roof of the measurement station 4 m above the ground through a probe with an air blower. The diameter of the probe was large, 50 mm, and the flow through it was large, so losses were estimated to be minimal. A smaller flow was separated from the sample and diluted with a bridge diluter with a dilution ratio of 8.2. The bridge diluter was especially designed for very small particles with minimized particle losses and the dilution ratio was determined before the field measurements in a laboratory experiment with sodium chloride particles. A similar diluter was used in e.g. Rönkkö et al. (2017). After the bridge diluter, the diluted sample was conducted to the instruments in the order presented in Fig. 1. The sampling lines were kept as short as possible in order to minimize diffusion losses.

During the measurement campaign, the particle size distributions, temperature and concentrations of CO_2, $PM_{2.5}$, PM_{10} and NO_X were also continuously measured at the station. The particle size distributions were measured from 6 to 800 nm with a differential mobility particle sizer (DMPS) consisting of an Airmodus CPC A20 and a Vienna type DMA. The sample for the DMPS was conducted through a separate sampling line before the bridge diluter. A single DMPS scan lasted 8 min. CO_2 concentration was measured with a LI-COR LI-7000 gas analyzer, $PM_{2.5}$ and PM_{10} with Thermo TEOM 1405 monitors and NO_X with a Horiba APNA-370 monitor. In this study, the NCA is studied with respect to CO_2 and particle size distribution. The diurnal variations of $PM_{2.5}$, PM_{10} and NO_X concentrations on weekdays are presented in Fig. 2a. The NO/NO_X ratio is also plotted for indicating the aging of the traffic-originated aerosol. Fig. 2b presents the diurnal variation of temperature and wind speed during the measurement campaign. During the measurements, the hourly averaged concentrations of NO varied from 0 to 132 μ m^{-3}, NO_2 from 2.5 to 97 μ m^{-3}, PM_{10} between 0 and 148 μ m^{-3}, and $PM_{2.5}$ from 0 to 22 μ m^{-3}. Temperature varied from −1.5 to 22 °C and wind speed from 0.3 to 3.8 m s^{-1}.

The measured concentrations and distributions were classified according to wind direction that indicates the direction from which the air sample was heading to the station. The wind direction data used in this study were measured at Pasila weather station approximately 700 m from the measurement station on the roof of an apartment building 53 m above the ground level. Fig. 3 presents the locations of the stations and the classified wind direction sectors. Because of the vortex affecting the average flow field in a street canyon, the wind direction at the measurement station was considered opposite to the direction above the roofs (Ahmad et al., 2005). Thus the wind was classified as coming to the station directly from the road when the wind direction measured at Pasila station was in range of 165–285 °, whereas wind from angles 0–105 ° and 345–360 ° was considered as coming from the opposite background direction. In this study, these two wind sectors are referred to as road and background sectors for clarity and consistency with other studies, though the terms do not describe this urban measurement environment quite correctly. It is also notable that here the term background refers to urban background air.

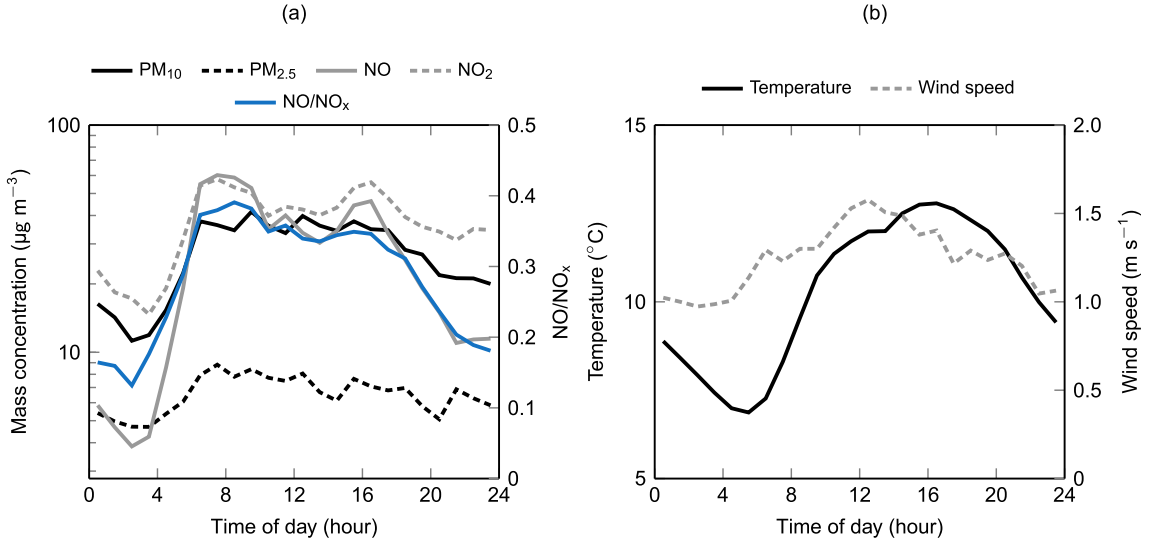

Fig. 2. (a) Diurnal variations of NO, NO_2, PM_{10}, $PM_{2.5}$ and the NO/NO_X ratio on weekdays during the measurement campaign. Note the logarithmic scale of the left y-axis. (b) Diurnal variation of temperature and wind speed during the measurement campaign.

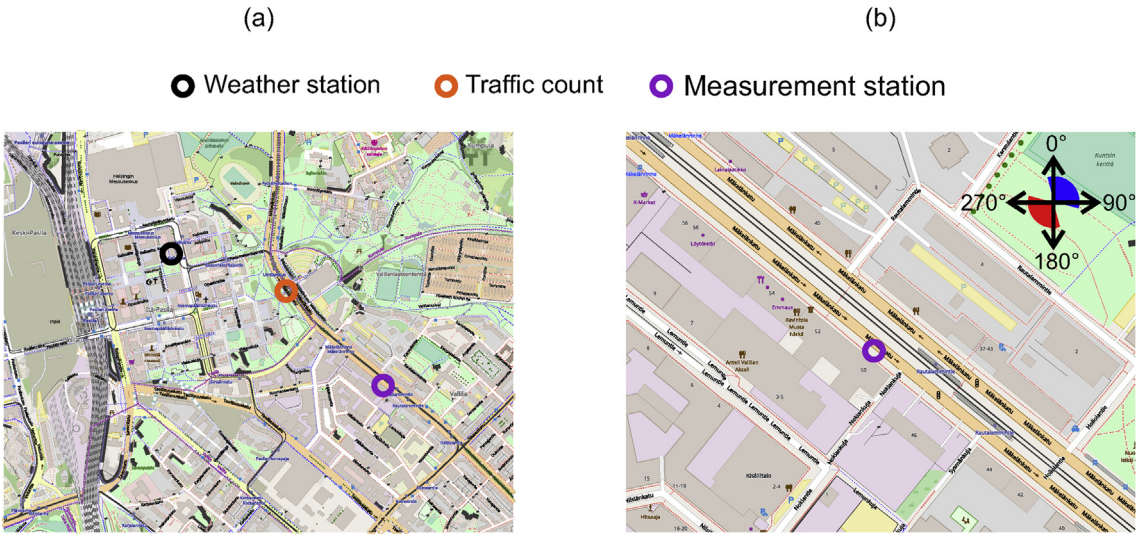

Fig. 3. Maps of the measurement locations. (a) Locations of the traffic count, the Pasila weather station and the measurement station, (b) the surroundings of the measurement station and the wind direction sectors used throughout this study on the map. © OpenStreetMap contributors.

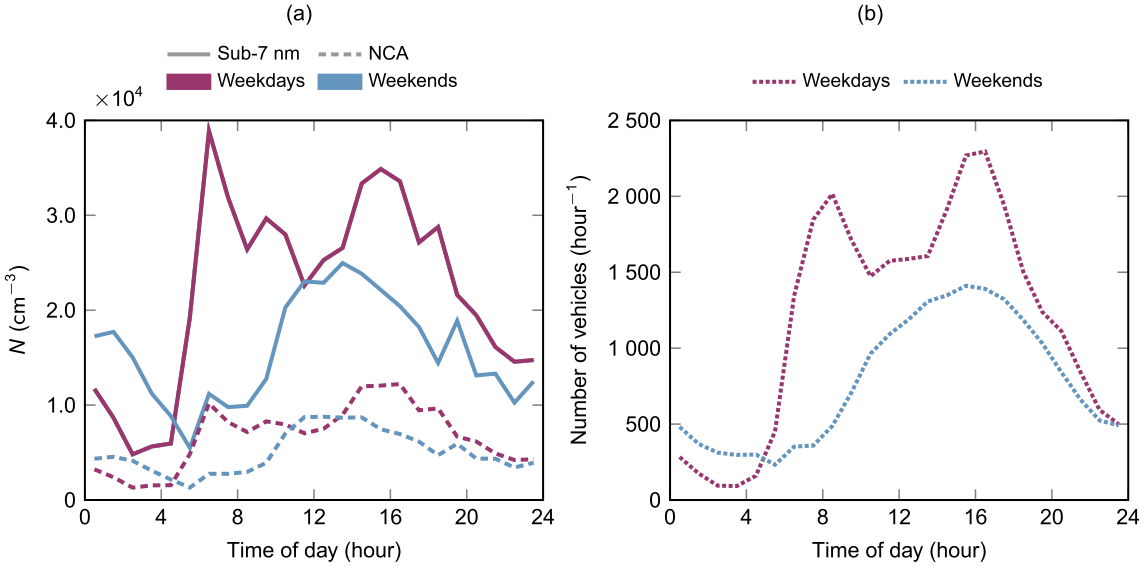

Fig. 4. (a) Average diurnal variations of the nanocluster aerosol (NCA, dashed line) and sub-7 nm particle (solid line) concentrations separately for weekdays and weekends. (b) Average diurnal variation of traffic (vehicles hour^{-1}) along the street Mäkelänkatu during the measurement campaign. The traffic count point was located in an intersection near the measurement station. Traffic data from the City of Helsinki.

3. Results and discussion

The impact of traffic on the NCA number concentration was studied from two aspects, both by comparing concentration data with simultaneous wind direction data and observing diurnal variations separately on weekends and weekdays. The pattern of traffic is clearly visible in Fig. 4, where diurnal variations of NCA and sub-7 nm particle concentrations during weekdays and weekends are shown. All wind directions have been included in this Figure. Diurnal variations were calculated from hourly averaged PSM and CPC data. On weekdays, both NCA and sub-7 nm concentrations rose during rush hours in the morning and around 4 pm and decreased in the night, whereas at weekends concentrations were low in the morning and achieved their highest values at midday. On weekday nights there was less traffic than on weekend nights, which can be seen in the concentrations.

In Fig. 5, wind direction was taken into consideration and diurnal variations of sub-7 nm particles and NCA on weekdays were calculated separately for two wind direction sectors. Data from times when wind was weak were also included in the analysis, since the wind speed did not affect the results noticeably. In the figure, the red color identifies data from times when wind was blowing to the measurement station from the road while the blue color presents times with wind blowing from the opposite background direction. Concentrations were plotted as relative to the total number concentration, i.e. the data of the PSM. Also the diurnal variation of the condensation sink was calculated for both wind directions from the size distributions measured with a DMPS and plotted in the same figure. The condensation sink was calculated with properties of sulphuric acid as presented in e.g. Pirjola et al. (1999). As can be seen from the figure, the NCA concentration in the road sector rose in the afternoon when the condensation sink decreased. In the morning the number of NCA particles in the air was restricted through faster condensation. The concentrations in the background sector presumably originated from more distant regions, so the condensation sink caused by fresh traffic-originated aerosol did not affect them as notably.

The relative number concentrations of sub-7 nm particles and NCA averaged over 15 min are presented as a function of wind direction in

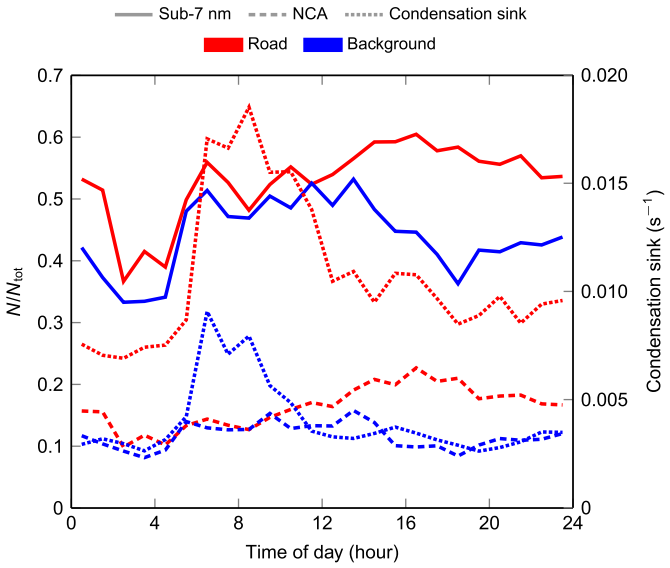

Fig. 5. Relative diurnal variations of the nanocluster aerosol (NCA) and sub-7 nm particle concentrations in two wind direction sectors on weekdays. Red color presents wind blowing from the road to the measurement station, blue from the opposite background direction. For comparison, diurnal variation of the condensation sink calculated from differential mobility particle sizer (DMPS) distributions is also included.

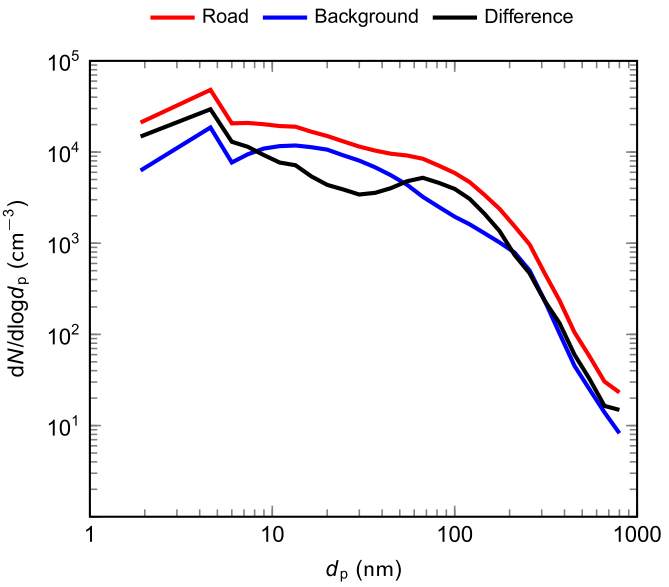

Fig. 7. Average particle size distributions from two wind direction sectors, road and background, and the difference of these wind sector distributions. Distributions consist of differential mobility particle sizer (DMPS) distributions from 6 to 800 nm and two smaller size classes calculated from the data of the particle size magnifier (PSM) and condensation particle counters (CPCs).

Fig. 6a and b, respectively. Data from times when traffic flow was low were excluded from the Figure. Wind directions were again classified into the road and background sectors. Data points belonging to the road sector were drawn with red color, background sector with blue and other wind directions with gray. In this figure, the effect of traffic is again evident, as the fractions of the NCA and sub-7 nm particles were at their highest when wind was blowing directly from the road and at their lowest in the background sector. The relative fraction of NCA varied with wind direction more than the relative fraction of sub-7 nm particles.

The relative fraction of NCA in a street canyon environment seemed to vary between 10% and 20%, which is less than 20%–54% measured in a semi-urban environment next to a larger road (Rönkkö et al., 2017). If the NCA originates from sulphuric acid, the difference in NCA fractions could be explained through differences in driving modes and engine load on the roads (Arnold et al., 2012). Another possibility is that the traffic-originated aerosol is more aged in a street canyon than near larger roads with no obstacles around, which results in smaller NCA concentrations.

3.1. Particle size distributions

In addition to the total number concentrations, also the particle size distribution was measured during the whole campaign. The studied size distributions were formed from the measurement data by combining DMPS scans with two extra size bins presenting the NCA and 3–7 nm

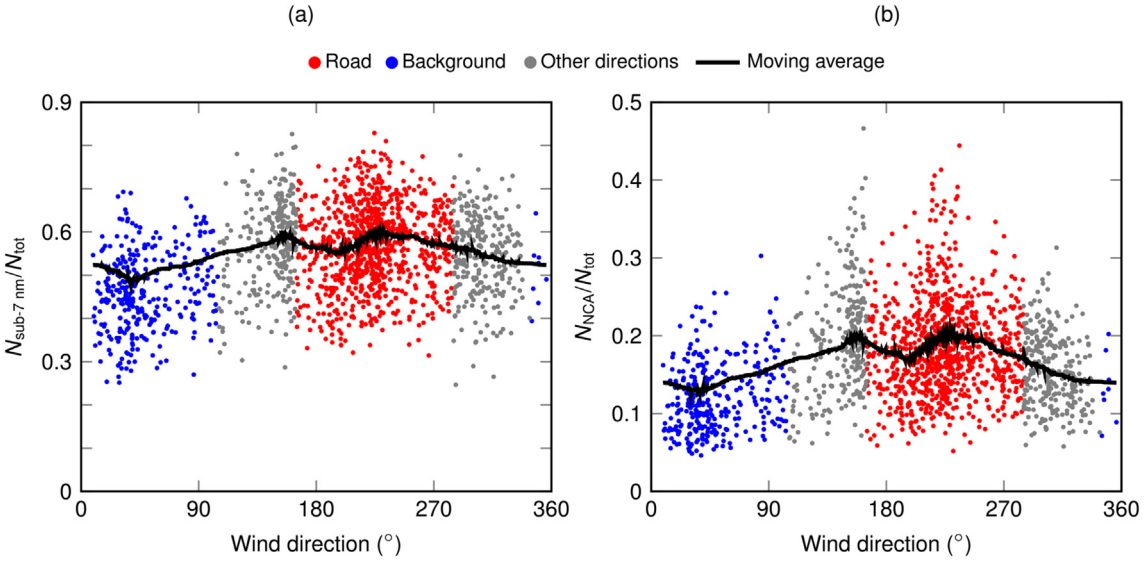

Fig. 6. The concentrations of (a) sub-7 nm particles and (b) nanocluster aerosol (NCA) relative to total particle number concentration as a function of wind direction. Each data point is an average over 15 min and black line presents the moving average with respect to wind direction. Data periods with low traffic flow have been excluded. Wind directions classified as coming from the road are colored with red, background directions with blue and other directions with gray. Note the different scales of the y-axes.

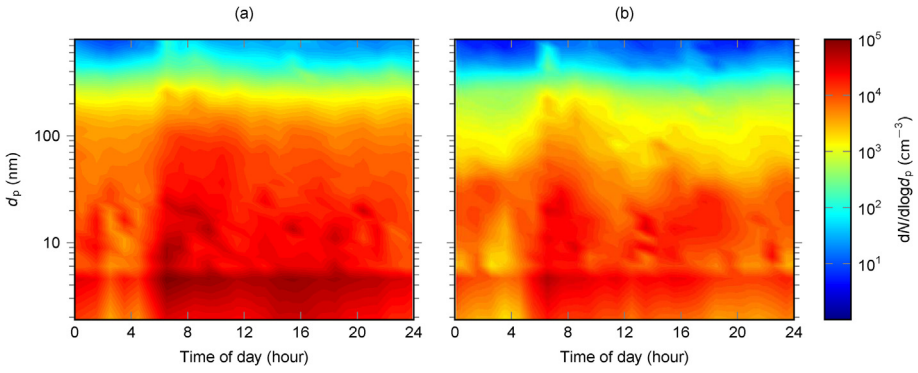

Fig. 8. Diurnal variation of particle size distributions on weekdays with wind blowing from the road (a) and from the background direction (b).

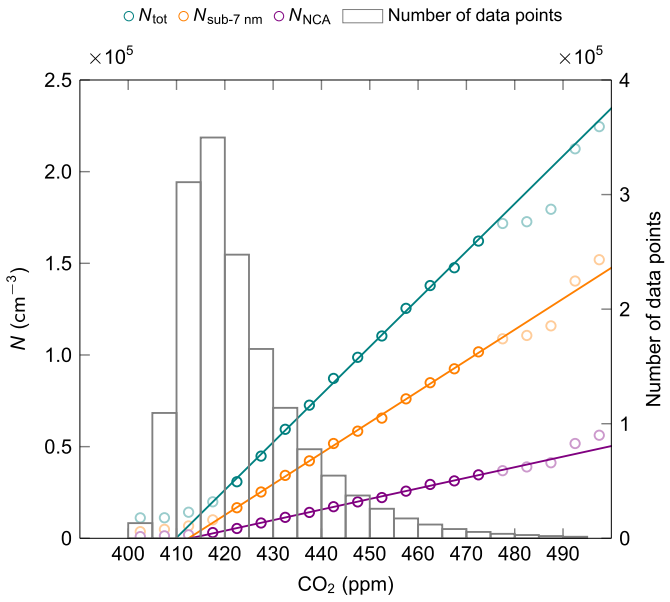

Fig. 9. Total particle number concentration and the concentrations of sub-7 nm particles and nanocluster aerosol (NCA) as a function of simultaneously measured CO_2 concentration. Data points are averages of number concentrations in 5 ppm CO_2 intervals. Number of averaged data points in each CO_2 interval is presented as a histogram. Points averaged from less than 5000 data points and those considered as background were excluded from linear fits and plotted with lighter colors. (For interpretation of the references to color in this figure legend, the reader is referred to the Web version of this article.)

particle concentrations calculated from the data of the PSM and CPCs. The size distributions were studied from the same two aspects as the number concentrations, through wind direction and diurnal variation. Fig. 7 presents averaged particle size distributions on weekdays from the whole measurement time with wind direction classification similar to preceding figures. The difference between the road and background distributions is plotted with black and approximately presents the particle number distribution from the traffic. Concentrations of all particle sizes were smaller in the background sector than when wind was blowing from the road. Especially in the smallest size bins the difference between these two wind sectors was significant. In the background sector, the nucleation and the accumulation modes were at greater particle sizes compared with the road sector. Based on the size distribution data, the concentration of NCA seemed to correlate well with the lower end of the DMPS size distribution and the nucleation mode. There appeared to be a separate mode for the NCA, but the interpretation of a separate mode based on this kind of cumulative concentration measurement with several instruments can only be tentative. It is reasonable that the two-modal shape of the size distribution was especially distinguished in the difference between the road and background distributions. The nucleation mode and accumulation mode have previously been observed in several roadside and urban on-road measurements (Kittelson et al., 2004; Virtanen et al., 2006; Pirjola et al., 2012). The accumulation mode mainly consists of soot particles originated from diesel engines and the nucleation mode particles are usually formed during the rapid dilution in ambient air. However, there can also be other types of particles such as lubricant oil originated particles (Rönkkö et al., 2014) or other non-volatile particles (Rönkkö et al., 2007) in the size range of both of these modes.

When DMPS distributions combined with the two extra size classes were averaged for each hour of a day, diurnal variations of particle size distributions were obtained. Fig. 8a presents distributions on weekdays from times when wind was blowing directly from the road whereas Fig. 8b shows data on weekdays with wind blowing from the background sector, so two contrary situations can be compared and the influence of traffic can be studied. The decrease of condensation sink seen in Fig. 5 during the day was clearly connected to the decrease of the mean particle size in the accumulation mode seen in Fig. 8b.

3.2. Emission factors

Measured particle number concentrations were compared to simultaneous CO_2 measurement data in order to calculate emission factors for all particles (N_{tot}), sub-7 nm particles and NCA. In this study, the emission factors represent the influence of traffic immediately at the roadside where aerosol is not assumed to correspond to tailpipe aerosol or to be very diluted. Thus when calculating the emission factors the particles are assumed to disperse as CO_2. However, the exhaust aerosol is not assumed to remain unchanged and it may undergo changes such as condensation and new particle formation during the dispersion and rapid dilution. Therefore, the diurnal variation of emission factors was analyzed in this study, for example, with respect to the changes in the condensation sink.

Fig. 9 presents measured particle number concentrations as a function of the CO_2 concentration. Particle concentrations were averaged over 5 ppm CO_2 intervals and the number of averaged data points in each interval is presented as a histogram in the figure. Points averaged from less than 5000 data points along with points classified as background were plotted with lighter colors and were excluded from linear fits calculated for data.

Emission factors were calculated from the slopes of the fits by assuming NTP conditions and using the value 3141 g kg_{fuel}^{-1} as the emission factor of CO_2 (Yli-Tuomi et al., 2005). Confidence intervals for obtained emission factors were calculated similarly from the 95% confidence bounds of the fits. Resulting emission factors and 95% confidence intervals for all particles, sub-7 nm particles and NCA were $4.22 \cdot 10^{15} \pm 0.11 \cdot 10^{15}$ kg_{fuel}^{-1}, $2.73 \cdot 10^{15} \pm 0.06 \cdot 10^{15}$ kg_{fuel}^{-1}, and $9.36 \cdot 10^{14} \pm 0.22 \cdot 10^{14}$ kg_{fuel}^{-1}, respectively.

When only weekday data was considered and emission factors were

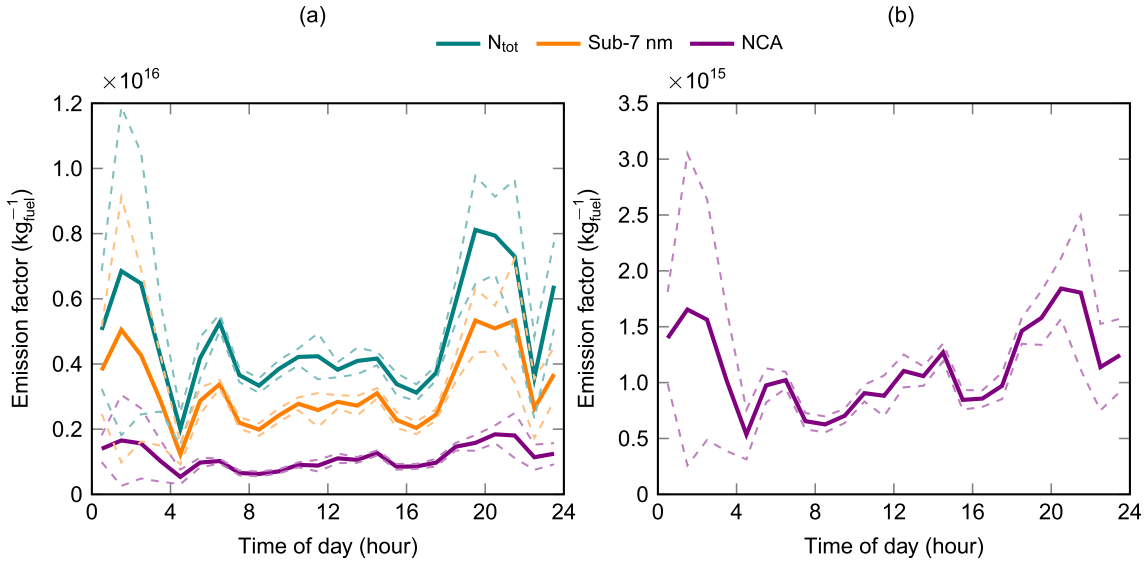

Fig. 10. (a) Diurnal variation of emission factors of nanocluster aerosol (NCA), sub-7 nm particles and all particles. (b) Diurnal variation of NCA emission factors presented more closely. Dashed lines in both figures present the 95% confidence bounds.

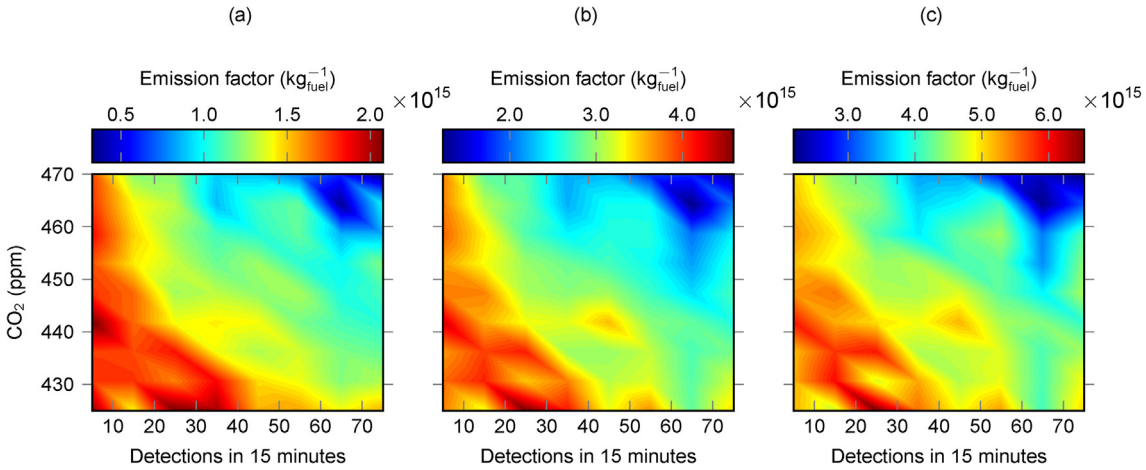

Fig. 11. Emission factors of (a) nanocluster aerosol (NCA), (b) sub-7 nm and (c) all particles as a function of CO_2 concentration and the number of detections in 15-minute time periods. Note different scales in color axis.

calculated separately for each hour of a day in a similar way to that used for the whole data, the diurnal variation of emission factors could be studied. The emission factors plotted in Fig. 10 seemed to increase in the evening and had higher values in the night than during the day. In the night, when there was less traffic and thus fewer data points with CO_2 values above the background level, it would be expected that the emission factors would have more deviation due to uncertainty. However, the results showed that the actual emission factors increased and not just the deviation, which was seen especially in the evening.

There appear to be several plausible explanations for an increase in particle emission factors at night. One possibility is a change in vehicle fleet composition, for which data are not available. However, particle emission factors for petrol and diesel fuelled vehicles differ substantially (Beddows and Harrison, 2008), leading to variations in the average composite emission factor with time of day. The second plausible explanation is that particle emission factors, especially for the semi-volatile component, are temperature-dependent, and increase at night when temperature is lower as Fig. 2b shows. Hussein et al. (2006) showed the dependence of particles of <100 nm in urban air upon temperature, showing an increase of two to three-fold as air temperature falls from 280 K to 250 K. Similarly Olivares et al. (2007) reported an increase from 150 particles per picogram of NO_X at 288 K to 380 particles per picogram of NO_x at 258 K. The fact that the emission factors of the NCA showed a similar trend to those of sub-7 nm and N_{tot} in Fig. 10 is an indication of their semi-volatile nature. The third possibility relates to the lower condensation sink at night, shown clearly in Fig. 5, or a combination of this with an increased tendency to condensation at a lower ambient temperature. A further possibility is differences in driving situations. NCA presumably correlates with gaseous sulphuric acid and as was discussed with Fig. 5, gaseous sulphuric acid increases as the engine load increases (Arnold et al., 2012). One affecting factor may be wind speed, because as Fig. 2b presents, wind was weaker at night than during the day, though the difference was not significant.

The variation of the emission factors was further studied by dividing measured concentration time series into 15-minute periods. As an example, one period was on 16.5.2017 at 10:00:00–10:15:00. The CO_2 concentrations in each period were classified into 5 ppm CO_2 intervals excluding the CO_2 values close to the background value. From the measured CO_2 data points during our example period were thus separated those between 425 and 430 ppm, those between 430 and 435 ppm etc. Calculating the number of data points in each CO_2 interval and in each time period gave the number of detections in 15 min, i.e. a kind of detection density for each CO_2 interval. If during our example period

there were 12 data points with CO_2 values between 425 and 430 ppm, we have now one data point, 12 detections in 15 min, in the CO_2 interval 425–430 ppm. The obtained quantity, detections in 15 min, for each CO_2 interval was further averaged over intervals of 10 detections. For example, the particle number concentrations of all the data points in the CO_2 interval 425–430 ppm and with 10–20 detections in 15 min were averaged, including our example data point. Emission factors were then calculated for these averaged data points from each CO_2 and detection interval using fixed background values for CO_2 and particle concentrations. The background values were determined from the whole data from the point where particle concentration begins to increase as a function of CO_2 in Fig. 9. One emission factor would then be calculated from our example data point, i.e. from the average particle number concentration of the data points with CO_2 in range 425–430 ppm and with 10–20 detections in 15 min. Finally, all of the emission factors calculated this way could be plotted as a function of both CO_2 concentration and the number of detections in 15-minute time periods in Fig. 11.

Fig. 11a, b and c for NCA, sub-7 nm particles and all particles, respectively, confirm that the emission factors were higher when there were fewer detections of high CO_2 concentrations. That situation occurred for example in the night when there was less traffic and CO_2 concentrations mostly stayed at the background level. During the rush hours, on the other hand, there were considerably more vehicles emitting CO_2, so high CO_2 values were detected more often. According to Fig. 11, emission factors were then lower, which can be seen in Fig. 10b as well.

4. Conclusions

The work reported in this paper is consistent with the earlier observations reported by Rönkkö et al. (2017) but amplified in a number of aspects. Careful analysis according to wind sector and time of day showed a very clear association of NCA with road traffic activity, and road traffic emissions as indicated by concentrations of larger particles.

The diurnal variation in NCA showed considerable similarity to that of total sub-7 nm particles. Also the size distribution data indicated that the NCA correlates with the nucleation mode particles also observable in the size range around 10 nm. While the diurnal variation in particles showed some similarity to the pattern of traffic activity, they were not identical and this may be reflective in part of changes to the vehicle fleet composition or typical driving situations throughout the day.

Emission factors for the NCA and sub-7 nm particles were reported and showed an increase at nighttime. While this may be linked to changes in traffic composition or driving conditions, i.e. to higher speed, this study links it more directly to a reduction in condensation sink or an increase in the driving force for particle formation by condensation due to reduced temperatures. However, it should be kept in mind that all of these reasons (changes in traffic composition, driving conditions, condensation sink and ambient temperature) can potentially increase the NCA and sub-7 nm particle emission. These aspects will require further research for their complete elucidation.

Acknowledgements

This study was funded by Tekes - the Finnish Funding Agency for Innovation (Grant 2883/31/2015), Helsinki Region Environmental Services Authority (HSY) and Pegasor Oy through the Cityzer project. The traffic count data from the road Mäkelänkatu were provided by Petri Blomqvist, City Environment Sector, Traffic and street planning, The City of Helsinki.

References

Ahmad, K., Khare, M., Chaudhry, K.K., 2005. Wind tunnel simulation studies on dispersion at urban street canyons and intersections – a review. J. Wind Eng. Ind. Aerod. 93, 697–717.

Alam, M.S., Zeraati-Rezaei, S., Stark, C.P., Liang, Z., Xu, H., Harrison, R.M., 2016. The characterisation of diesel exhaust particles – composition, size distribution and partitioning. Faraday Discuss 189, 69–84.

Alanen, J., Saukko, E., Lehtoranta, K., Murtonen, T., Timonen, H., Hillamo, R., Karjalainen, P., Kuuluvainen, H., Harra, J., Keskinen, J., Rönkkö, T., 2015. The formation and physical properties of the particle emissions from a natural gas engine. Fuel 162, 155–161.

Arnold, F., Pirjola, L., Rönkkö, T., Reichl, U., Schlager, H., Lähde, T., Heikkilä, J., Keskinen, J., 2012. First online measurements of sulfuric acid gas in modern heavy-duty diesel engine exhaust: Implications for nanoparticle formation. Environ. Sci. Technol. 46, 11227–11234.

Beddows, D.C., Harrison, R.M., 2008. Comparison of average particle number emission factors for heavy and light duty vehicles derived from rolling chassis dynamometer and field studies. Atmos. Environ. 42, 7954–7966.

Biswas, S., Ntziachristos, L., Moore, K.F., Sioutas, C., 2007. Particle volatility in the vicinity of a freeway with heavy-duty diesel traffic. Atmos. Environ. 41, 3479–3493.

Haywood, J., Boucher, O., 2000. Estimates of the direct and indirect radiative forcing due to tropospheric aerosols: a review. Rev. Geophys. 38, 513–543.

Hussein, T., Karppinen, A., Kukkonen, J., Härkönen, J., Aalto, P.P., Hämeri, K., Kerminen, V.M., Kulmala, M., 2006. Meteorological dependence of size-fractionated number concentrations of urban aerosol particles. Atmos. Environ. 40, 1427–1440.

Iida, K., Stolzenburg, M., McMurry, P., 2009. Effect of working fluid on sub-2 nm particle detection with a laminar flow ultrafine condensation particle counter. Aerosol. Sci. Technol. 43, 81–96.

Kirchner, U., Scheer, V., Vogt, R., Kägi, R., 2009. TEM study on volatility and potential presence of solid cores in nucleation mode particles from diesel powered passenger cars. J. Aerosol Sci. 40, 55–64.

Kirkby, J., Duplissy, J., Sengupta, K., Frege, C., Gordon, H., Williamson, C., Heinritzi, M., Simon, M., Yan, C., Almeida, J., Trostl, J., Nieminen, T., Ortega, I., Wagner, R., Adamov, A., Amorim, A., Bernhammer, A.-K., Bianchi, F., Breitenlechner, M., Brilke, S., Chen, X., Craven, J., Dias, A., Ehrhart, S., Flagan, R., Franchin, A., Fuchs, C., Guida, R., Hakala, J., Hoyle, C., Jokinen, T., Junninen, H., Kangasluoma, J., Kim, J., Krapf, M., Kurten, A., Laaksonen, A., Lehtipalo, K., Makhmutov, V., Mathot, S., Molteni, U., Onnela, A., Peräkylä, O., Piel, F., Petäjä, T., Praplan, A., Pringle, K., Rap, A., Richards, N., Riipinen, I., Rissanen, M., Rondo, L., Sarnela, N., Schobesberger, S., Scott, C., Seinfeld, J., Sipila, M., Steiner, G., Stozhkov, Y., Stratmann, F., Tomé, A., Virtanen, A., Vogel, A., Wagner, A., Wagner, P., Weingartner, E., Wimmer, D., Winkler, P., Ye, P., Zhang, X., Hansel, A., Dommen, J., Donahue, N., Worsnop, D., Baltensperger, U., Kulmala, M., Carslaw, K., Curtius, J., 2016. Ion-induced nucleation of pure biogenic particles. Nature 533, 521–526.

Kittelson, D., Watts, W., Johnson, J., 2004. Nanoparticle emissions on Minnesota highways. Atmos. Environ. 38, 9–19.

Kontkanen, J., Lehtipalo, K., Ahonen, L., Kangasluoma, J., Manninen, H.E., Hakala, J., Rose, C., Sellegri, K., Xiao, S., Wang, L., Qi, X., Nie, W., Ding, A., Yu, H., Lee, S., Kerminen, V.-M., Petäjä, T., Kulmala, M., 2017. Measurements of sub-3 nm particles using a particle size magnifier in different environments: from clean mountain top to polluted megacities. Atmos. Chem. Phys. 17, 2163–2187.

Kulmala, M., Kerminen, V.-M., 2008. On the formation and growth of atmospheric nanoparticles. Atmos. Res. 90, 132–150.

Kulmala, M., Mordas, G., Petäjä, T., Grönholm, T., Aalto, P.P., Vehkamäki, H., Hienola, A.I., Herrmann, E., Sipilä, M., Riipinen, I., Manninen, H.E., Hämeri, K., Stratmann, F., Bilde, M., Winkler, P.M., Birmili, W., Wagner, P.E., 2007a. The condensation particle counter battery (CPCB): a new tool to investigate the activation properties of nanoparticles. J. Aerosol Sci. 38, 289–304.

Kulmala, M., Riipinen, I., Sipilä, M., Manninen, H., Petäjä, T., Junninen, H., Dal Maso, M., Mordas, G., Mirme, A., Vana, M., Hirsikko, A., Laakso, L., Harrison, R., Hanson, I., Leung, C., Lehtinen, K., Kerminen, V.-M., 2007b. Toward direct measurement of atmospheric nucleation. Science 318, 89–92.

Kumar, P., Ketzel, M., Vardoulakis, S., Pirjola, L., Britter, R., 2011. Dynamics and dispersion modelling of nanoparticles from road traffic in the urban atmospheric environment – a review. J. Aerosol Sci. 42, 580–603.

Kuuluvainen, H., Rönkkö, T., Järvinen, A., Saari, S., Karjalainen, P., Lähde, T., Pirjola, L., Niemi, J., Hillamo, R., Keskinen, J., 2016. Lung deposited surface area size distributions of particulate matter in different urban areas. Atmos. Environ. 136, 105–113.

Lehtoranta, K., Murtonen, T., Vesala, H., Koponen, P., Alanen, J., Simonen, P., Rönkkö, T., Timonen, H., Saarikoski, S., 2017. Natural gas engine emission reduction by catalysts. Emission Control Sci. Technol. 3, 142–152.

Lelieveld, J., Evans, J.S., Fnais, M., Giannadaki, D., Pozzer, A., 2015. The contribution of outdoor air pollution sources to premature mortality on a global scale. Nature 525, 367–371.

Maher, B., Ahmed, I., Karloukovski, V., MacLaren, D., Foulds, P., Allsop, D., Mann, D., Torres-Jardon, R., Calderon-Garciduenas, L., 2016. Magnetite pollution nanoparticles in the human brain. Proc. Natl. Acad. Sci. U.S.A. 113, 10797–10801.

Monks, P., Granier, C., Fuzzi, S., Stohl, A., Williams, M., Akimoto, H., Amann, M., Baklanov, A., Baltensperger, U., Bey, I., Blake, N., Blake, R., Carslaw, K., Cooper, O., Dentener, F., Fowler, D., Fragkou, E., Frost, G., Generoso, S., Ginoux, P., Grewe, V., Guenther, A., Hansson, H., Henne, S., Hjorth, J., Hofzumahaus, A., Huntrieser, H., Isaksen, I., Jenkin, M., Kaiser, J., Kanakidou, M., Klimont, Z., Kulmala, M., Laj, P., Lawrence, M., Lee, J., Liousse, C., Maione, M., McFiggans, G., Metzger, A., Mieville, A., Moussiopoulos, N., Orlando, J., O'Dowd, C., Palmer, P., Parrish, D., Petzold, A., Platt, U., Pöschl, U., Prevot, A., Reeves, C., Reimann, S., Rudich, Y., Sellegri, K., Steinbrecher, R., Simpson, D., ten Brink, H., Theloke, J., van der Werf, G., Vautard, R., Vestreng, V., Vlachokostas, C., von Glasow, R., 2009. Atmospheric composition change – global and regional air quality. Atmos. Environ. 43, 5268–5350.

Nemmar, A., Hoet, P.H.M., Vanquickenborne, B., Dinsdale, D., Thomeer, M., Hoylaerts, M.F., Vanbilloen, H., Mortelmans, L., Nemery, B., 2002. Passage of inhaled particles into the blood circulation in humans. Circulation 105, 411–414.

Oberdörster, G., Oberdörster, E., Oberdörster, J., 2005. Nanotoxicology: an emerging discipline evolving from studies of ultrafine particles. Environ. Health Perspect. 113, 823–839.

Olivares, G., Johansson, C., Ström, J., Hansson, H.C., 2007. The role of ambient temperature for particle number concentrations in a street canyon. Atmos. Environ. 41, 2145–2155.

Pirjola, L., Kulmala, M., Wilck, M., Bischoff, A., Stratmann, F., Otto, E., 1999. Effects of aerosol dynamics on the formation of sulphuric acid aerosols and cloud condensation nuclei. J. Aerosol Sci. 30, 1079–1094.

Pirjola, L., Lähde, T., Niemi, J., Kousa, A., Rönkkö, T., Karjalainen, P., Keskinen, J., Frey, A., Hillamo, R., 2012. Spatial and temporal characterization of traffic emissions in urban microenvironments with a mobile laboratory. Atmos. Environ. 63, 156–167.

Pirjola, L., Rönkkö, T., Saukko, E., Parviainen, H., Malinen, A., Alanen, J., Saveljeff, H., 2017. Exhaust emissions of non-road mobile machine: real-world and laboratory studies with diesel and HVO fuels. Fuel 202, 154–164.

Pope III, C.A., Burnett, R.T., Thun, M.J., Calle, E.E., Krewski, D., Ito, K., Thurston, G.D., 2002. Lung cancer, cardiopulmonary mortality, and long-term exposure to fine particulate air pollution. J. Am. Med. Assoc. 287, 1132–1141.

Rönkkö, T., Kuuluvainen, H., Karjalainen, P., Keskinen, J., Hillamo, R., Niemi, J.V., Pirjola, L., Timonen, H.J., Saarikoski, S., Saukko, E., Järvinen, A., Silvennoinen, H., Rostedt, A., Olin, M., Yli-Ojanperä, J., Nousiainen, P., Kousa, A., Dal Maso, M., 2017. Traffic is a major source of atmospheric nanocluster aerosol. Proc. Natl. Acad. Sci. Unit. States Am. 114, 7549–7554.

Rönkkö, T., Lähde, T., Heikkilä, J., Pirjola, L., Bauschke, U., Arnold, F., Schlager, H., Rothe, D., Yli-Ojanperä, J., Keskinen, J., 2013. Effects of gaseous sulphuric acid on diesel exhaust nanoparticle formation and characteristics. Environ. Sci. Technol. 47, 11882–11889.

Rönkkö, T., Pirjola, L., Ntziachristos, L., Heikkilä, J., Karjalainen, P., Hillamo, R., Keskinen, J., 2014. Vehicle engines produce exhaust nanoparticles even when not fueled. Environ. Sci. Technol. 48, 2043–2050.

Rönkkö, T., Virtanen, A., Kannosto, J., Keskinen, J., Lappi, M., Pirjola, L., 2007. Nucleation mode particles with a nonvolatile core in the exhaust of a heavy duty diesel vehicle. Environ. Sci. Technol. 41, 6384–6389.

Rotstayn, L., Keywood, M., Forgan, B., Gabric, A., Galbally, I., Gras, J., Luhar, A., McTainsh, G., Mitchell, R., Young, S., 2009. Possible impacts of anthropogenic and natural aerosols on Australian climate: a review. Int. J. Climatol. 29, 461–479.

Sakurai, H., Tobias, H.J., Park, K., Zarling, D., Docherty, K.S., Kittelson, D.B., McMurry, P.H., Ziemann, P.J., 2003. On-line measurements of diesel nanoparticle composition and volatility. Atmos. Environ. 37, 1199–1210.

Sgro, L., Borghese, A., Speranza, L., Barone, A., Minutolo, P., Bruno, A., D'Anna, A., D'Alessio, A., 2008. Measurements of nanoparticles of organic carbon and soot in flames and vehicle exhausts. Environ. Sci. Technol. 42, 859–863.

Shi, J.P., Harrison, R.M., 1999. Investigation of ultrafine particle formation during diesel exhaust dilution. Environ. Sci. Technol. 33, 3730–3736.

Tobias, H.J., Beving, D.E., Ziemann, P.J., Sakurai, H., Zuk, M., McMurry, P.H., Zarling, D., Waytulonis, R., Kittelson, D.B., 2001. Chemical analysis of diesel engine nanoparticles using a nano-DMA/thermal desorption particle beam mass spectrometer. Environ. Sci. Technol. 35, 2233–2243.

Vanhanen, J., Mikkilä, J., Lehtipalo, K., Sipilä, M., Manninen, H.E., Siivola, E., Petäjä, T., Kulmala, M., 2011. Particle size magnifier for nano-CN detection. Aerosol. Sci. Technol. 45, 533–542.

Virtanen, A., Rönkkö, T., Kannosto, J., Ristimäki, J., Mäkelä, J., Keskinen, J., Pakkanen, T., Hillamo, R., Pirjola, L., Hämeri, K., 2006. Winter and summer time size distributions and densities of traffic-related aerosol particles at a busy highway in Helsinki. Atmos. Chem. Phys. 6, 2411–2421.

Xiao, S., Wang, M., Yao, L., Kulmala, M., Zhou, B., Yang, X., Chen, J., Wang, D., Fu, Q., Worsnop, D., Wang, L., 2015. Strong atmospheric new particle formation in winter in urban Shanghai, China. Atmos. Chem. Phys. 15, 1769–1781.

Yli-Tuomi, T., Aarnio, P., Pirjola, L., Mäkelä, T., Hillamo, R., Jantunen, M., 2005. Emissions of fine particles, NOx, and CO from on-road vehicles in Finland. Atmos. Environ. 39, 6696–6706.

Zhu, Y., Hinds, W., Kim, S., Shen, S., Sioutas, C., 2002. Study of ultrafine particles near a major highway with heavy-duty diesel traffic. Atmos. Environ. 36, 4323–4335.